Materials Science in Semiconductor Processing 151 (2022) 106997

Contents lists available at ScienceDirect

Materials Science in Semiconductor Processing

journal homepage: www.elsevier.com/locate/mssp

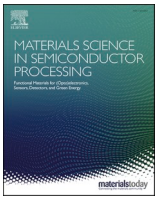

Complex impedance formalism: An alternative approach for exploration of relaxation dynamics in conductive materials

Yohandys A. Zulueta [a], Y. Leyet [b,c], F. Guerrero [c], J. Angada-Rivera [d], Minh Tho Nguyen [e], My-Phuong Pham-Ho [f,g,*]

[a] Departamento de Física, Facultad de Ciencias Naturales y Exactas, Universidad de Oriente, CP, 90500, Santiago de Cuba, Cuba
[b] LPMAT, Postgraduate Program in Materials Science and Engineering, Department of Materials Engineering, Federal University of Amazonas, Manaus, Amazonas, 69067-005, Brazil
[c] Postgraduate Program in Physics, Department of Physics, Federal University of Amazonas, Manaus, Amazonas, 69067-005, Brazil
[d] Federal Institute of Education, Science and Technology of Amazonas, Manaus, Amazonas, 69020-120, Brazil
[e] Institute for Computational Science and Technology (ICST), Ho Chi Minh City, 700000, Viet Nam
[f] Faculty of Chemical Engineering, Ho Chi Minh City University of Technology (HCMUT), 268 Ly Thuong Kiet Street, District 10, Ho Chi Minh City, 700000, Viet Nam
[g] Vietnam National University Ho Chi Minh City (VNU-HCM), Linh Trung Ward, Thu Duc District, Ho Chi Minh City, 700000, Viet Nam

ARTICLE INFO

Keywords:
Dielectric modulus
Ionic conduction
Relaxation dynamics
Impedance spectroscopy
Relaxation distribution function
Complex impedance formalism

ABSTRACT

A new method, the complex impedance formalism, is presented to disclose the relaxation process of conducting materials. This method is an extrapolation of the dielectric modulus formalism in the Bode representation of the impedance. As in the dielectric modulus formalism, the relaxation process can be approached in both the frequency and time domains for non-Debye relaxation type. The complex impedance formalism is tested by analysis of the relaxation process of the solid $BaTiO_3$ material at high temperatures. A combination of complex impedance and dielectric modulus formalism provides us with a better understanding concerning individual relaxation regions. The complex impedance formalism allows the hidden relaxation process at low frequency regime to be accessible, whereas the dielectric modulus formalism discloses the relaxation process at high frequency in mixed electronic-ionic conductors.

1. Introduction

Complex impedance spectroscopy is a powerful technique for characterization of the electrical behavior of materials [1–13]. This method allows to disclose the electrical phenomena occurring in a material and its interfaces with electronically conducting electrodes. It is used to emphasize the dynamic charge carriers in the interfacial regions or the bulk of ionic, semiconducting, insulator and mixed ionic-electronic materials. Electrical response data are commonly represented in terms of complex permittivity, dielectric modulus, impedance and admittance [1–9]. In the impedance representation [1–7], the response plotted in a complex plane represents a succession of semicircles (Nyquist plots) due to conducting regions in the system (grain, grain boundary).

Many important multifunctional compounds are actually the mixed electronic and ionic conductors [1,5–10]. Impedance spectroscopy for these materials can not only determine their electrical properties, but also demonstrate the relaxation dynamics occurred in the sample. In a typical Bode diagram, that is a plot of the impedance versus the frequency, a maximal value of the imaginary component of the impedance and the corresponding frequency is related to the relaxation time of the relaxation process existing in the sample [1–5]. Such a relaxation process occurs when the charge carriers fail to follow the frequency of the applied electric field. In this sense, the relaxation time is the required time for the charge carrier not to feel from the external electric field. Commonly, the relaxation time against temperature is a thermally activated process follows the conventional Arrhenius equation expressing the dependence of the rate of the relaxation process with respect to the activation energy.

There are various methods to explore electrical properties of mixed electronic-ionic materials [1,14,15]. In the alternate current (ac) conductivity representation, the dependence of the conductivity with respect to the frequency follows the universal Jonscher relation; by

* Corresponding author. Faculty of Chemical Engineering, Ho Chi Minh City University of Technology (HCMUT), 268 Ly Thuong Kiet Street, District 10, Ho Chi Minh City, 700000, Viet Nam.
E-mail address: phmphuong@hcmut.edu.vn (M.-P. Pham-Ho).

https://doi.org/10.1016/j.mssp.2022.106997
Received 31 May 2022; Accepted 24 July 2022
Available online 12 August 2022
1369-8001/

changing the temperature the Arrhenius dependence of the direct current (dc) conductivity can be determined [14]. The Jonscher model allows us to probe the electrical nature of a material, but not its relaxation process. By using the equivalent circuit method one can explore the electrical properties in each material region such as grain, interphase, grain boundary [4,5,10–13]. Both methods are well defined in the frequency domain. Another method is the dielectric modulus formalism where the electrical properties and relaxation process can be explored in time and frequency domains simultaneously [6,8,15] These methods, based on impedance spectroscopy measurements, have been used to report electrical properties and relaxation process in a variety of multifunctional materials, including semiconductors and battery materials [6–13].

It is known that the pure Bode diagram is not able to elucidate the relaxation process explicitly [9–13]. This is due to the lack of a formulation to describe the common non-Debye time-relaxation distribution function occurring in such mixed materials [6,15–24]. When the individual grain and grain boundary impedance responses are not well-resolved, a strategy to avoid large errors by fitting with equivalent circuit models is to elucidate the bulk resistance by plotting the imaginary part of the dielectric modulus versus frequency, and then extracting the frequency-peak position and the total resistance from the intercept of the real part of the impedance in a Nyquist plot [12,13]. As in the common Bode analysis, such a procedure does not reveal the relaxation process occurred in the sample.

In this context, we set out in the present work to propose and validate a formulation called the complex impedance formalism (CIF) whose main objective is to determine the relaxation process of samples from the Bode diagram. This new approach also describes the relaxation and conducting properties in both time and frequency domains simultaneously. In addition, it considers the material at low frequency where the grain contribution to the electrical properties is decisive. The proof of this new formalism is actually compared to the results obtained from the well-described dielectric modulus formalism which was applied to the relaxation process in the barium titanate ($BaTiO_3$) compound.

2. Methodology

In impedance spectroscopy the procedure consists in an application on the sample a voltage-sinusoidal signal (V_0) with an angular frequency ω, recording the current intensity I. The sample impedance is a complex function:

$$Z(\omega,T)=Z'(\omega,T)+iZ''(\omega,T)=|Z(\omega,T)|exp(i\varphi) \tag{1}$$

where $Z'(\omega,T)$, $Z''(\omega,T)$ are the real and imaginary component of $Z(\omega,T)$, respectively, φ the phase angle at the frequency ω and temperature T [1,2,15,20]. The electrical measurements can be expressed in term of the complex dielectric constant $\varepsilon(\omega,\ T)$, complex dielectric modulus $M(\omega,T)=\varepsilon(\omega,T)^{-1}$ or electric conductivity $\sigma(\omega,T)$ which are related to each other as follow:

$$\varepsilon(\omega,T)=[i\omega C_0 Z(\omega,T)]^{-1};\ M(\omega,T)=\ i\omega C_0 Z(\omega,T);\sigma(\omega,T)=i\omega\varepsilon_0\varepsilon(\omega,T) \tag{2}$$

where $C_0=\varepsilon_0 A/L$ is the geometric factor (L, A length and area of the sample, and $\varepsilon_0=8.854\times10^{-14}$ Fcm^{-1} being the standard permittivity). Equation (2) represents the relationship between the extensive magnitude $Z(\omega,T)$ with the intensive $\varepsilon(\omega,T)$, $M(\omega,T)$ y $\sigma(\omega,T)$. Each of the abovementioned intensive magnitudes can be expressed as:

$$A(\omega,T)=\ A'(\omega,T)+iA''(\omega,T) \tag{3}$$

with $A=\varepsilon,M$ o σ, respectively.

The conductivity relaxation dynamics of a material can be studied by using the well-known dielectric modulus formalism [6,15,19], which consists in the data conversion from impedance to the dielectric modulus by combining both equations (2) and (3). In our assumption, the formulations established for the dielectric modulus formalist can be expanded to the other intensive magnitudes as follow:

$$A(\omega,T)=A'(\omega,T)+A''(\omega,T)=A_\infty[1-F(\omega,T)] \tag{4}$$

where A_∞ is the real A component at high frequency. $F(\omega,T)$ distribution function of the relaxation time that describes the relaxation type of the sample. Of the various $F(\omega,T)$ described in the literature, the most popular formulations are:

$$F_{HN}(\omega,T)=[1+(i\omega\tau_{HN})^{\alpha}]^{-\gamma}\ \ \text{Havriliak}-\text{Negami}\ \ (\text{HN}) \tag{5}$$

$$F_{CD}(\omega,T)=[1+(i\omega\tau_{CD})]^{-\gamma}\ \ \text{Davidson}-\text{Cole}\ \ (\text{CD}) \tag{6}$$

$$F_{CC}(\omega,T)=[1+(i\omega\tau_{CD})^{\alpha}]^{-1}\ \ \text{Cole}-\text{Cole}\ \ (\text{CC}) \tag{7}$$

where τ_j ($j=HN,\ CD$ and CC) relaxation time of each $F(\omega,T)$ type and α and γ are empirical parameters ranging between 0 and 1 [8,15,21,22].

In the time domain (t) the A magnitude is expressed as [15,21,22]:

$$A(\omega,T)=A_\infty\left[1-\int_0^{+\infty}\left(-\frac{d\Phi}{dt}\right)exp(-i\omega t)dt\right] \tag{8}$$

where Φ the relaxation function in the time domain [15,21].

If $F(\omega,T)=F_{HN}(\omega,T)$ the distribution function $\rho(\tau)$ of the relaxation time τ, is:

$$\rho(\tau)=\frac{1}{\pi}\frac{\left(\frac{\tau}{\tau_{HN}}\right)^{\alpha\gamma}\sin(\gamma\theta)}{\left[\left(\frac{\tau}{\tau_{HN}}\right)^{2\alpha}+2\left(\frac{\tau}{\tau_{HN}}\right)^{\alpha}\cos(\alpha\pi)+1\right]^{\frac{\gamma}{2}}} \tag{9}$$

where:

$$\theta=\tan^{-1}\left|\frac{\sin(\alpha\pi)}{\left(\frac{\tau}{\tau_{HN}}\right)^{\alpha}+\cos(\alpha\pi)}\right| \tag{10}$$

By using $\rho(\tau)$, the derivative of Φ in the frequency is obtained directly [15,21]:

$$d\Phi(\omega)\Big/d\tau=\int_0^{+\infty}[\rho(\tau)/(1+\omega\tau)]d\tau \tag{11}$$

And in the time domain as:

$$\Phi(t)=\int_0^{+\infty}\rho(\tau)\exp(-t/\tau)d\tau \tag{12}$$

When $F(\omega,T)\ =F_{CD}(\omega,T)$, we thus have [15,21]:

$$\frac{d\Phi(t)}{dt}=\frac{1}{\Gamma(\beta)\tau_{CD}}\left(\frac{t}{\tau_{CD}}\right)^{\beta-1}exp(-t/\tau_{CD}) \tag{13}$$

When $F(\omega,T)=F_{CC}(\omega,T)$, we then have [15,21]:

$$g_{CC}(\ln\tau)=\frac{1}{2\pi}\frac{\sin(\alpha\pi)}{\cosh\left[\alpha\ln\left(\frac{t}{\tau_{CC}}\right)+\cos(\alpha\pi)\right]} \tag{14}$$

Consequently, in the Cole-Cole relaxation function in the time domain can be expressed as:

$$\Phi(t)=\int_0^{\infty}g_{CC}(\ln\tau)exp(-t/\tau)d(\ln\tau);g_{CC}(\ln\tau)=\frac{1}{2\pi}\frac{\sin(\alpha\pi)}{\cosh\left[\alpha\ln\left(\frac{t}{\tau_{CC}}\right)+\cos(\alpha\pi)\right]} \tag{15}$$

which it is fitted to the Kolhrausch-Williams-Watts (KWW) type

[19–23]:

$$\Phi(t) = exp(-t/\tau)^{\beta} \tag{16}$$

where β is a non-dimensional parameter ranging between 0 and 1 and it is related to the correlated jumps of the charge carriers respect to its vicinity. As a matter of fact, when β tends to 0 then the correlation is getting strong [19–23]. The average relaxation time, defined as the required time by the charge carriers to diffuse through the conduction path, is expressed as:

$$< \tau >= \tau\Gamma(1/\beta)/\beta \tag{17}$$

where Γ is the Euler's Gamma function.

It is well-known that both relaxation and conduction processes are thermally activated. The magnitudes $< \tau >$, σ or τ can be plotted vs the temperature T to obtain the activation energy E_a by fitting with the Arrhenius (standardized) dependence type [14,15]:

$$\Theta(T) = \exp\left(-\frac{E_a}{k_B T}\right) \tag{18}$$

where $\Theta(T) = < \tau >$, σ o τ, and k_B the Boltzmann constant.

Using the formulation described here, the approach to study both the relaxation and conducting properties of a conductive material follows various steps, including:

1. The choice of the temperature range of study.
2. A plot of A'' versus frequency ω. If it is an appreciable, maximum then this method is applicable; otherwise, it is advisable to use other approaches such as equivalent circuits or Jonscher model [14].
3. Fitting the experimental data with the best distribution relaxation function given in equations (5)–(7), recording the parameters α, γ and τ for each temperature.
4. Transform the data and fitting with KWW dependence equation to obtain β, τ and $< \tau >$ by using equations (16) and (17).
5. Arrhenius dependence type $\ln[\Theta(T)]$ vs. 1/T to obtain E_a from equation (18).

This procedure allows the relaxation and conducting properties at both time and frequency domain to be investigated simultaneously. The steps 2 and 3 refer to the frequency domain and the step 4 to the time domain. Note that the recipe of the dielectric modulus formalism is obtained by replacing $A'' = M''$ and the new procedure namely complex impedance formalism is when $A'' = Z''$. The advantage in employing the complex impedance formalism is that this method inherits the performance of the dielectric modulus formalism (being able to study transport properties and relaxation in time and frequency domains), and that it is not necessary to transform the experimental data form impedance to modulus, thereby introducing less uncertainty during the analysis of the data. Therefore, under the assumption of the three intensive magnitudes described in equation (3), by replacing $A'' = \varepsilon''(\omega, T)$ or $\sigma''(\omega, T)$ we can further propose two alternative methods, but in fact both parameters $\varepsilon''(\omega, T)$ and $\sigma''(\omega, T)$ are obtained from the measurable impedance data.

3. Results and discussions

3.1. Behavior of the relaxation times in the frequency domain

The polymeric precursor method was experimentally used to obtain the $BaTiO_3$ sample; details of the experimental conditions can be found in our previous work [8,24]. The dielectric characterization of the material was carried out by impedance spectroscopy using a HP-4194 spectrometer at temperatures ranging in between 298 and 953 K, at intervals of 10 K, and frequencies between 100 Hz and 10 MHz.

Fig. 1 displays dependence of the imaginary impedance and dielectric modulus component with the frequency. These curves are adjusted by the best relaxation distribution function. We now start fitting with the Havriliak-Negami distribution function because it is the most general one whereas the others are applied for particular cases. After fitting, Fig. 1a is described by the Cole-Cole type, whereas the Davidson-Cole describes the behavior of the dielectric modulus.

In Fig. 1a, the magnitude of Z'' decreases and its correspondent maximum-frequency position increases with increasing temperature, highlighting a decrease of the resistivity of the material. The shifting of Z'' peaks towards higher frequency, together with the observable asymmetric broadening point out that the relaxation time decreases with the increase of temperature and the presence of activated relaxation process. Similarly, for the M'' the maximum frequency position increase from 10^4 to 10^6 Hz while the peaks become higher with the increment of temperature.

Comparing the frequency maximum positions of both methods, the relaxation times in the frequency domain appear to be different. In the complex impedance formalism, the relaxation times obtained by the fitting ranges between 10^{-5} -10^{-3} s, whereas for the dielectric modulus approach lies between 10^{-7} -10^{-6} s. These findings, together with the peak tendencies described above, are indicators for the presence of thermally activated process [6–9,16–21].

With the results of the previous fitting in the frequency domain, the

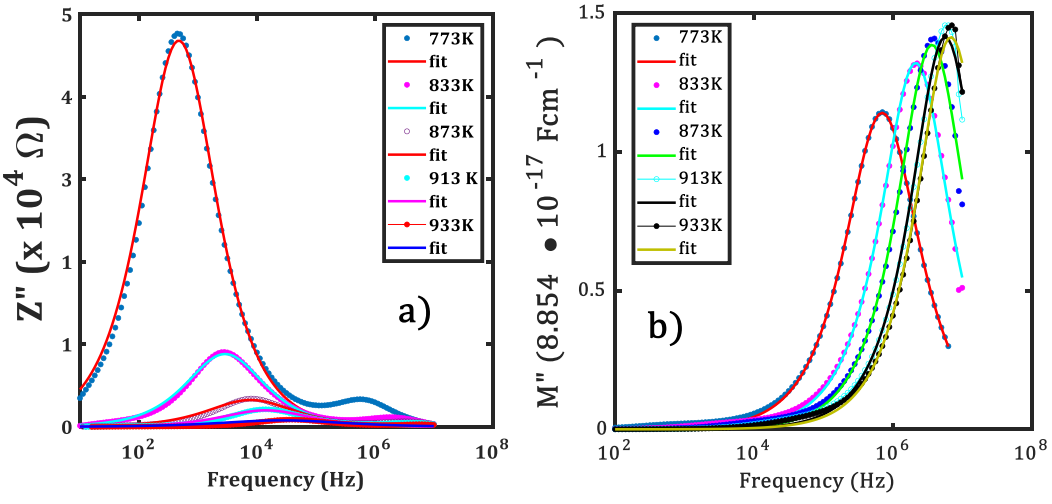

Fig. 1. Frequency dependence of the imaginary component of a) the impedance and b) dielectric modulus at different temperatures of barium titanate.

relaxation distribution function is obtained in the time domain by using equations (13) and (14). Fig. 2 shows the normalized relaxation distribution function Φ(t) in the time domain for different temperatures. Equation (14) is used or the impedance formalism (cf. Fig. 2a), and equation (13) for the dielectric modulus method (cf. Fig. 2b). The abscissa position of the saddle point is related to the relaxation time in the time domain [6,8,15,21]. These curves are fitted to the KWW function to obtain the relaxation time at each temperature in the time domain, including the β parameter.

It is appreciable that the separation between the curves for the impedance formalism is larger than those for the dielectric modulus method. By standing at the saddle point meaning, the relaxation time in the time domain decreases with the increment of temperature. After fitting using the KWW, the relaxation time ranges between 10^{-5}-10^{-3} s for the impedance and 10^{-7}-10^{-6} s for the dielectric modulus formalisms, respectively, in agreement with the results derived from the frequency domain discussed above.

With the values of the relaxation time in the time domain and the β parameter, the average relaxation time (being the required time for the charge carrier to make an effective jump successively, contributing to the conductivity) is computed by using equation (17).

The dependence on the temperature of the relaxation time in the frequency domain and the average relaxation time (in the time domain by definition) for both impedance and dielectric modulus formalisms are depicted in Fig. 3a and b, respectively. In both formalisms, the relaxation time decreases with the increment of the temperature, and are close to each other, indicating the involvement of thermally activated processes and the ionic character of the $BaTiO_3$ structure [6,8,15,21].

The tendency of the β, α or γ parameters with temperature is depicted in the figures inset. For the impedance formalism, β decreases from 0.84 to 0.7 and the Cole-Cole parameter α from 0.84 to 0.55 with the T increment. This means that the correlation between the charge carriers becomes stronger. In the dielectric modulus formalism, β remains constant near of 0.9, (and γ oscillating between 0.95 and 0.98) indicating independent jumps on their local environment contributing to the conduction process in this temperature range [8,15,21].

Fig. 4a shows the Arrhenius dependence of the average relaxation time of both methods. From the slope of log(<τ>) versus 1/T, the activation energy can be obtained. For the impedance formalism, the magnitude of <τ> is in an order superior as compared to those from the dielectric modulus approach. The activation energy derived in such a way amounts to 1.80 and 0.88 eV from both impedance and modulus formalisms, respectively.

Guo et al. [25] and Yang and coworkers [26] reported values of activation energy ranging between 0.99 and 1.55 eV for micro- and nanocrystalline $BaTiO_3$ samples including electrical core-shell microstructure. These authors attributed such values to the oxidation enthalpy, *p*-type conductivity in these samples. Leyet and coworkers reported an activation energy of 0.8 eV [8]. In this context, the 0.88 eV value is attributable to oxygen vacancy mechanism, whereas the higher value of 1.80 eV is more adequate for electronic conduction (*n*- or *p*-type conductivity) [1,6,8,13,25]. These facts reveal that the combination of CIF and DMF is a good strategy to study the relaxation process in the entire frequency range of electric measurements, in addition to the relaxation analysis in the time domain.

The microscopic activation energy, defined as $E_a^m(T) = \beta(T)E_a$, is included in Fig. 4b. In each temperature and formalism, the E_a^m value is lower than the global E_a. With the T increment, E_a^m tends to decrease slightly, reaffirming the presence of a thermally activated process.

Considering the results obtained above, the main observation in the Z'' versus frequency plots is the presence of asymmetric peaks broadening with increase of temperature. Several authors reported these findings of Z'' spectrum in other mixed materials [4,5,9], attributing them to the existence of thermally activated process and relaxation phenomenon [4,5,9,16–18]. However, none of previous reports described the relaxation process in term of relaxation distribution function. For instance, Dash and coworkers [16] reported the electrical properties of Li_2TiO_3 by using impedance spectroscopy measurements, and described qualitatively the phenomenon in term of Z'' and M'' versus frequency and the electrical properties were disclosed by other well-known method, including the Jonscher equation. Zakuan and coworkers [17] used only the relation of the characteristic frequency, derived from the peak abscissa position at each temperature, to obtain the relaxation time and the activation energy of Li_2TiO_3. It has been reported that the shifting towards higher frequencies as temperature increases of the Z'' peaks can be associated to the presence of a non-Debye behavior relaxation process at the grain boundary region [27].

As for an understanding of the origin of such differences of the Z'' and M'' spectra, Fig. 5 depicts a combined plot of both M'' and Z'' versus frequency. According to the extrinsic nature of the dielectric behavior of $BaTiO_3$, the internal layer barrier capacitor model explains the dielectric tendency of this material [3,28–30]. In accordance with this model, Z'' dominates the most resistive part of the sample, i.e., the grain boundary and the most capacitive part (the grain) is dominated and characterized by M'' [3,17]. Taking a closer look into Fig. 5, the low frequency region is dominated by Z'' as a response of the insulating grain boundary region while the high frequency response in M'' is due to semiconducting grain

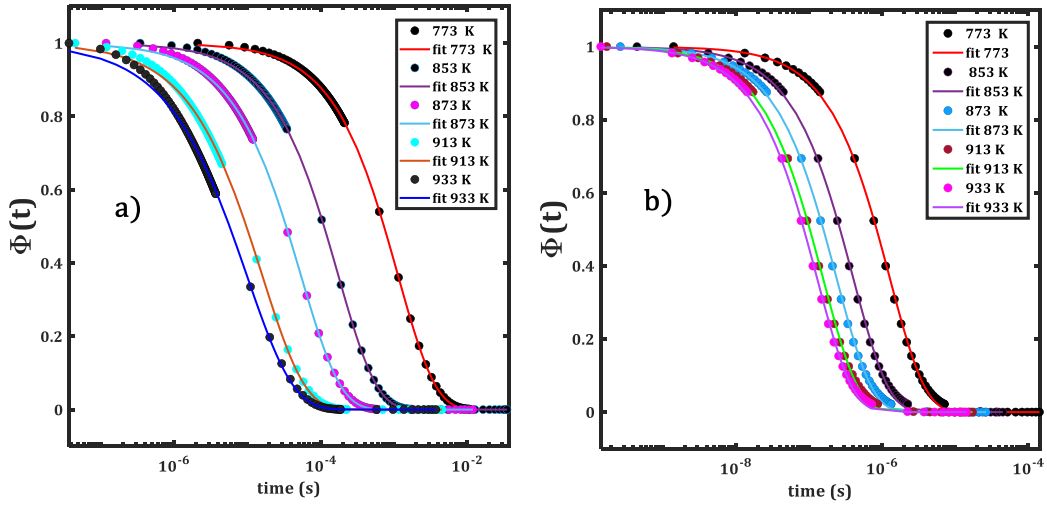

Fig. 2. Relaxation distribution function in the time domain obtained from a) CIF and b) DMF methods for different temperatures. Lines represent the KWW fitting.

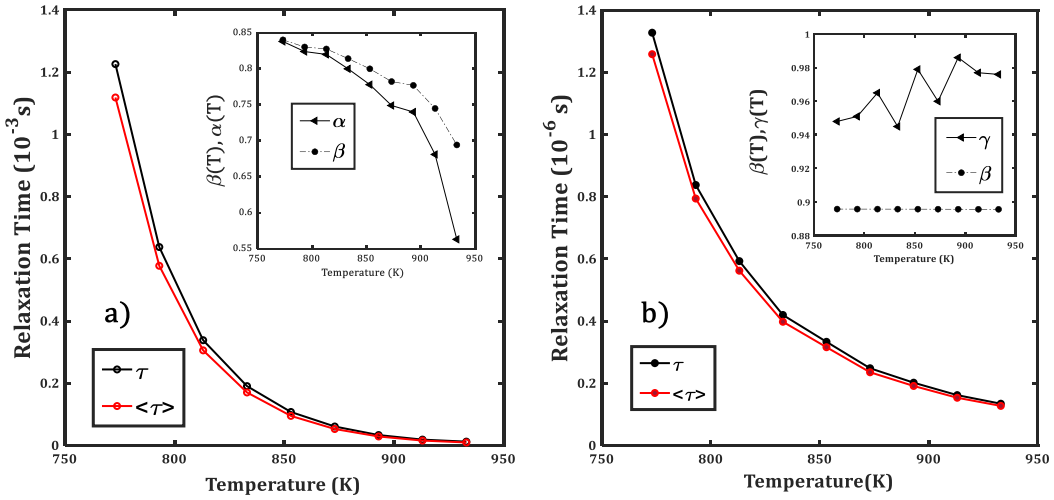

Fig. 3. Temperature dependence of the average relaxation time <τ> and the relaxation time in the frequency domain τ obtained from a) impedance and b) dielectric modulus formalisms. Figures insets depict the temperature variation of correlation parameters.

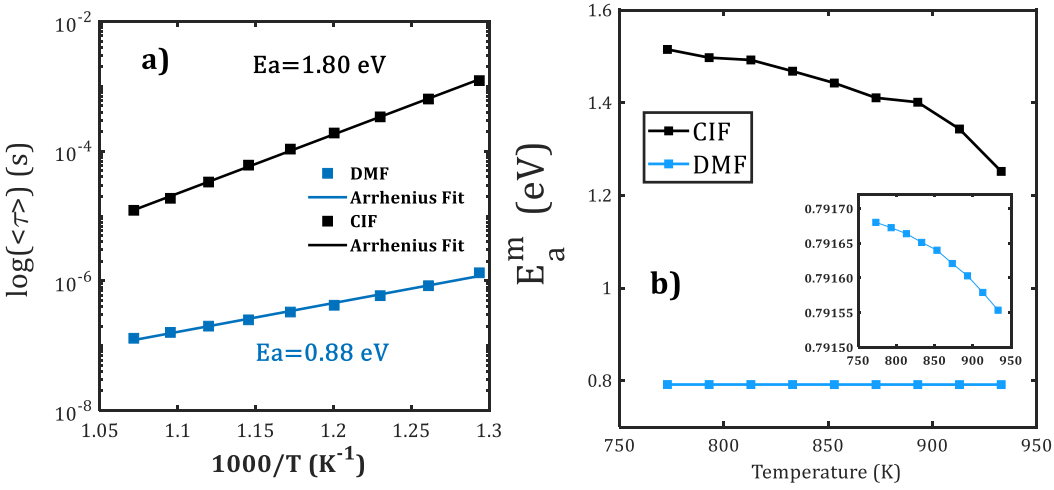

Fig. 4. a) Arrhenius dependence of relaxation time and **b)** temperature evolution of the microscopic activation energy obtained by both complex impedance (CIF) and dielectric modulus (DMF) formalisms.

[28–31].

A mismatch between M'' and Z'' spectra on the frequency scale is clearly observed, which implies that the charge carrier movement is not fully a long-range characteristic [3,30]. The M'' and Z'' peaks separation coincides with the differences encountered in the relaxation time derived from both M'' and Z'' formalisms. A similar behavior is observed for the rest of the temperature range.

In summary, while the complex impedance formalism quantifies the relaxation process occurring at the grain boundary region, the dielectric modulus formalism describes the relaxation process at the grain. A combination of both formalisms provides a complementary understanding of the active process in each relaxation region (grain and grain boundary). In the case of $BaTiO_3$, it is clear that the existence of such relaxation region in the sample, evidenced by the differences on relaxation time, the relaxation function distribution and activation energy. For instance, a Cole-Cole type relaxation function is well adjusted to the impedance spectra in the temperature range studied, while for the dielectric modulus formalism, having lower relaxation times and activation energy, a Davidson-Cole type describes well the relaxation process. There are two main relaxation processes, a storage or short-ranged migration of the charge carriers at low frequency, and a large-scale migration of the charge carriers at high frequency. In this sense, in combining the complex impedance and dielectric modulus formalisms, a comprehensive study of the relaxation process in the frequency and time domain simultaneously in each relaxation region (grain and grain boundary) can be achieved.

4. Conclusions

A new approach to study the relaxation processes in conductive materials was presented. The proposed method, names as complex impedance formalism, consists in the extension of the well-known dielectric modulus formalism by taking directly the impedance measurements. This method takes the advantages from the dielectric modulus formalism where the relaxation process can be studied in both time and frequency domains and useful for non-Debye relaxation type. The present approached was tested by an analysis of the relaxation process of the $BaTiO_3$ solid material at high temperatures where the relaxation process occurs. The complex impedance formalism exposes explicitly the relaxation distribution type for the first time. Our results reveal that a combined study using both formalisms can provide us with more comprehensive understanding on the individual relaxation

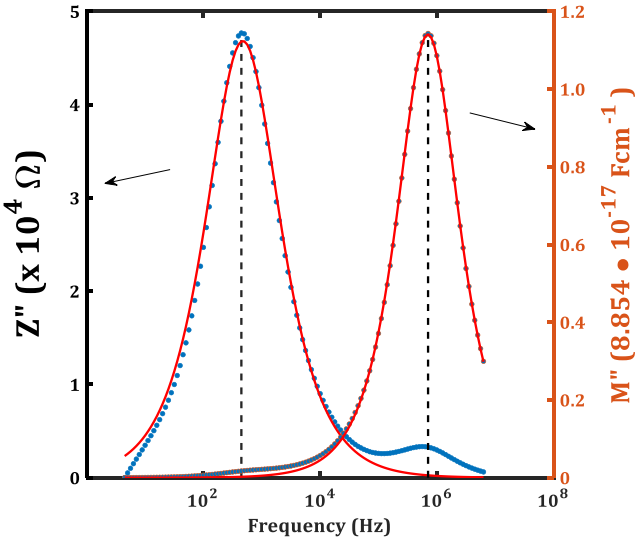

Fig. 5. Combined plots of M″ and Z″ against frequency at 773 K. Dashed lines are eye guidelines of the relaxation peaks of Z″ and M″, red line represent the fitting.

regions, both grain and grain boundary.

As the dielectric modulus formalism is mainly used to study the relaxation process at high frequency regime in ionic conductors, the method proposed here allows us to access to the hidden relaxation process at low frequency regime where generally the charge carrier accumulation or short-range motion is expected.

This work provides to the research community a powerful tool to identify and quantify the relaxation process in mixed electronic-ionic conductors, including semiconductors.

CRediT authorship contribution statement

Yohandys A. Zulueta: Conceptualization, Investigation, Methodology. **Y. Leyet:** Data curation, Supervision, Validation. **F. Guerrero:** Data curation, Validation, Writing – review & editing. **J. Angada-Rivera:** Data curation, Supervision, Validation. **Minh Tho Nguyen:** Supervision, Writing – review & editing. **My-Phuong Pham-Ho:** Conceptualization, Writing – original draft, Writing – review & editing.

Declaration of competing interest

The authors declare that they have no known competing financial interests or personal relationships that could have appeared to influence the work reported in this paper.

Acknowledgements

We acknowledge the Ho Chi Minh City University of Technology (HCMUT), Vietnam National University VNU-HCM for supporting this study.

References

[1] S. Lee, C.A. Randall, Determination of electronic and ionic conductivity in mixed ionic conductors: HiTEC and in-situ impedance spectroscopy analysis of isovalent and aliovalent doped $BaTiO_3$, Solid State Ionics 249–250 (2013) 86–92, https://doi.org/10.1016/j.ssi.2013.07.016.

[2] D.D. MacDonald, Reflections on the history of electrochemical impedance spectroscopy, Electrochim. Acta 51 (2006) 1376–1388, https://doi.org/10.1016/j.electacta.2005.02.107.

[3] Q. Liu, J. Liu, D. Lu, W. Zheng, Colossal dielectric behavior and relaxation in Nd-doped $BaTiO_3$ at low temperature, Ceram. Int. 44 (2018) 7251–7258, https://doi.org/10.1016/j.ceramint.2018.01.181.

[4] C. Lenser, N.H. Menzler, Impedance characterization of supported oxygen ion conducting electrolytes, Solid State Ionics 334 (2019) 70–81, https://doi.org/10.1016/j.ssi.2019.01.031.

[5] U. Dash, S. Sahoo, S.K.S. Parashar, P. Chaudhuri, Effect of Li+ ion mobility on the grain boundary conductivity of Li_2TiO_3 nanoceramics, J. Adv. Ceram. 3 (2014) 98–108, https://doi.org/10.1007/s40145-014-0098-9.

[6] Y.A. Zulueta, J.A. Dawson, Y. Leyet, J. Anglada-Rivera, F. Guerrero, R.S. Silva, M. T. Nguyen, Consequences of Ca multisite occupation for the conducting properties of $BaTiO_3$, J. Solid State Chem. 243 (2016) 77–82, https://doi.org/10.1016/j.jssc.2016.08.013.

[7] A. Singh, M.K. Shamim, S. Sharma, R. Rai, Effect of different microwave power applied during microwave assisted radiant heating on the structure, dielectric and electrical properties of $Ba_{0.8}Ca_{0.2}TiO_3$ ceramics, J. Mater. Sci. Mater. Electron. 29 (2018) 8158–8166, https://doi.org/10.1007/s10854-018-8821-x.

[8] Y. Leyet, F. Guerrero, J.P. de la Cruz, Relaxation dynamics of the conductive processes in $BaTiO_3$ ceramics at high temperature, Mater. Sci. Eng. B Solid-State Mater. Adv. Technol. 171 (2010) 127–132, https://doi.org/10.1016/j.mseb.2010.03.085.

[9] L.P. Teo, M.H. Buraidah, A.F.M. Nor, S.R. Majid, Conductivity and dielectric studies of Li_2SnO_3, Ionics 18 (2012) 655–665, https://doi.org/10.1007/s11581-012-0667-2.

[10] M. Bruch, L. Millet, J. Kowal, M. Vetter, Novel method for the parameterization of a reliable equivalent circuit model for the precise simulation of a battery cell's electric behavior, J. Power Sources 490 (2021), 229513, https://doi.org/10.1016/j.jpowsour.2021.229513.

[11] P. Iurilli, C. Brivio, V. Wood, On the use of electrochemical impedance spectroscopy to characterize and model the aging phenomena of lithium-ion batteries: a critical review, J. Power Sources 505 (2021), 229860, https://doi.org/10.1016/j.jpowsour.2021.229860.

[12] F. Yang, P. Wu, D.C. Sinclair, Suppression of electrical conductivity and switching of conduction mechanisms in "stoichiometric" $(Na_{0.5}Bi_{0.5}TiO_3)_{1-x}(BiAlO_3)_x$ ($0 \leq x \leq 0.08$) solid solutions, J. Mater. Chem. C 5 (2017) 7243–7252, https://doi.org/10.1039/c7tc02519j.

[13] F. Yang, P. Wu, D.C. Sinclair, Electrical conductivity and conduction mechanisms in $(Na_{0.5}Bi_{0.5}TiO_3)_{1-x}(BiScO_3)_x$ ($0.00 \leq x \leq 0.25$) solid solutions, J. Mater. Chem. C 6 (2018) 11598–11607, https://doi.org/10.1039/c8tc04679d.

[14] A.K. Jonscher, Dielectric relaxation in solids, J. Phys. D Appl. Phys. 32 (1999), https://doi.org/10.1088/0022-3727/32/14/201. R57–R70.

[15] C. León, M.L. Lucía, J. Santamaría, F. Sánchez-Quesada, Universal scaling of the conductivity relaxation in crystalline ionic conductors, Phys. Rev. B 57 (1998) 41–44, https://doi.org/10.1103/PhysRevB.57.41.

[16] U. Dash, S. Sahoo, P. Chaudhuri, S.K.S. Parashar, K. Parashar, Electrical properties of bulk and nano Li_2TiO_3 ceramics: a comparative study, J. Adv. Ceram. 3 (2014) 89–97, https://doi.org/10.1007/s40145-014-0094-0.

[17] N.S. Zakuan, H.J. Woo, L.P. Teo, M.Z. Kufian, Z. Osman, Li_2SnO_3 anode synthesized via simplified hydrothermal route using eco-compatible chemicals for lithium-ion battery, J. Electrochem. Soc. 166 (2019), https://doi.org/10.1149/2.0091912jes. A2341–A2348.

[18] A. Lakshmi-Narayana, O.M. Hussain, A. Mauger, C. Julien, Transport properties of nanostructured Li_2TiO_3 anode material synthesized by hydrothermal method, Science 1 (2019) 56, https://doi.org/10.3390/sci1030056.

[19] P. Dzwonkowski, M. Eddrief, C. Julien, M. Balkanski, Electrical a.c. conductivity of $B2O_{3x}Li_2O$ glass thin films and analysis using the electric modulus formalism,

Mater. Sci. Eng. B 8 (1991) 193–200, https://doi.org/10.1016/0921-5107(91)90038-W.
[20] K. Miyano, M. Yanagida, Y. Shirai, Impedance spectroscopy revisited, Adv. Energy Mater. 10 (2020), 1903097, https://doi.org/10.1002/aenm.201903097.
[21] C. Léon, A. Rivera, A. Várez, J. Sanz, J. Santamaria, K.L. Ngai, Origin of constant loss in ionic conductors, Phys. Rev. Lett. 86 (2001) 1279–1282, https://doi.org/10.1103/PhysRevLett.86.1279.
[22] Y. Feldman, A. Puzenko, Y. Ryabov, Non-Debye dielectric relaxation in complex materials, Chem. Phys. 284 (2002) 139–168, https://doi.org/10.1016/S0301-0104(02)00545-1.
[23] A. Rivera-Calzada, K. Kaminski, C. Leon, M. Paluch, Ion dynamics under pressure in an ionic liquid, J. Phys. Chem. B 112 (2008) 3110–3114, https://doi.org/10.1021/jp710479b.
[24] Y.A. Zulueta, J.A. Dawson, Y. Leyet, F. Guerrero, J. Anglada-Rivera, M.T. Nguyen, The potential existence of mixed defect incorporation modes for rare-earth doped cubic $BaTiO_3$, Phys. Status Solidi Basic Res. 253 (2016) 733–737, https://doi.org/10.1002/pssb.201552329.
[25] X. Guo, C. Pithan, C. Ohly, C.L. Jia, J. Dornseiffer, F.H. Haegel, R. Waser, Enhancement of p -type conductivity in nanocrystalline $BaTiO_3$ ceramics, Appl. Phys. Lett. 86 (2005), 082110, https://doi.org/10.1063/1.1864232.
[26] H. Yang, Z. Lu, L. Li, W. Bao, H. Ji, J. Li, A. Feteira, F. Xu, Y. Zhang, H. Sun, Z. Huang, W. Lou, K. Song, S. Sun, G. Wang, D. Wang, I.M. Reaney, Novel $BaTiO_3$-based, Ag/Pd-compatible lead-free relaxors with superior energy storage performance, ACS Appl. Mater. Interfaces 12 (2020) 43942–43949, https://doi.org/10.1021/acsami.0c13057.
[27] L.P. Teo, Impedance spectroscopy analysis of Li_2SnO_3, Ionics 23 (2017) 309–317, https://doi.org/10.1007/s11581-016-1899-3.
[28] D.C. Sinclair, T.B. Adams, F.D. Morrison, A.R. West, $CaCu_3Ti_4O_{12}$: one-step internal barrier layer capacitor, Appl. Phys. Lett. 80 (2002) 2153–2155, https://doi.org/10.1063/1.1463211.
[29] D.C. Sinclair, A.R. West, Impedance and modulus spectroscopy of semiconducting $BaTiO_3$ showing positive temperature coefficient of resistance, J. Appl. Phys. 66 (1989) 3850–3856, https://doi.org/10.1063/1.344049.
[30] A.K. Dubey, P. Singh, S. Singh, D. Kumar, O. Parkash, Charge compensation, electrical and dielectric behavior of lanthanum doped $CaCu_3Ti_4O_{12}$, J. Alloys Compd. 509 (2011) 3899–3906, https://doi.org/10.1016/j.jallcom.2010.12.156.
[31] F.D. Morrison, D.C. Sinclair, A.R. West, An alternative explanation for the origin of the resistivity anomaly in La-doped $BaTiO_3$, J. Am. Ceram. Soc. 84 (2001) 474–476, https://doi.org/10.1111/j.1151-2916.2001.tb00684.x.